

Article

# Hyperactive RAS/PI3-K/MAPK Signaling Cascade in Migration and Adhesion of *Nf1* Haploinsufficient Mesenchymal Stem/Progenitor Cells

Yuan Zhou <sup>1,2,3,†,\*</sup>, Yongzheng He <sup>2,3,†</sup>, Richa Sharma <sup>3</sup>, Wen Xing <sup>1,2,3</sup>, Selina A. Estwick <sup>2,3</sup>, Xiaohua Wu <sup>2,3</sup>, Steven D. Rhodes <sup>3</sup>, Mingjiang Xu <sup>2,3</sup> and Feng-Chun Yang <sup>2,3</sup>

<sup>1</sup> State Key Laboratory of Experimental Hematology, Institute of Hematology and Blood Diseases Hospital, Chinese Academy of Medical Sciences and Peking Union Medical College, Tianjin 300020, China; E-Mail: xw2318@aliyun.com

<sup>2</sup> Department of Pediatrics, Indiana University School of Medicine, Indianapolis, IN 46202, USA; E-Mails: yonhe@iu.edu (Y.H.); selinaorlando@yahoo.com (S.A.E.); wu\_xiaohua@lilly.com (X.W.); mx2@iupui.edu (M.X.); fyang@iu.edu (F.-C.Y.)

<sup>3</sup> Herman B Wells Center for Pediatric Research, Indiana University School of Medicine, Indianapolis, IN 46202, USA; E-Mails: ricsharm@iupui.edu (R.S.); sdrhodes@iupui.edu (S.D.R.)

† These authors contributed equally to this work.

\* Author to whom correspondence should be addressed; E-Mail: yuanzhou@ihcams.ac.cn; Tel.: +86-22-2390-9166; Fax: +86-22-2390-9025.

Academic Editor: Irmgard Tegeder

Received: 9 January 2015 / Accepted: 13 May 2015 / Published: 1 June 2015

---

**Abstract:** Neurofibromatosis type 1 (NF1) is an autosomal dominant disease caused by mutations in the *NF1* tumor suppressor gene, which affect approximately 1 out of 3000 individuals. Patients with NF1 suffer from a range of malignant and nonmalignant manifestations such as plexiform neurofibromas and skeletal abnormalities. We previously demonstrated that *Nf1* haploinsufficiency in mesenchymal stem/progenitor cells (MSPCs) results in impaired osteoblastic differentiation, which may be associated with the skeletal manifestations in NF1 patients. Here we sought to further ascertain the role of *Nf1* in modulating the migration and adhesion of MSPCs of the *Nf1* haploinsufficient (*Nf1*<sup>+/-</sup>) mice. *Nf1*<sup>+/-</sup> MSPCs demonstrated increased nuclear-cytoplasmic ratio, increased migration, and increased actin polymerization as compared to wild-type (WT) MSPCs.

Additionally, *Nf1*<sup>+/-</sup> MSPCs were noted to have significantly enhanced cell adhesion to fibronectin with selective affinity for CH271 with an overexpression of its complimentary receptor, CD49e. *Nf1*<sup>+/-</sup> MSPCs also showed hyperactivation of phosphoinositide 3-kinase (PI3-K) and mitogen activated protein kinase (MAPK) signaling pathways when compared to WT MSPCs, which were both significantly reduced in the presence of their pharmacologic inhibitors, LY294002 and PD0325901, respectively. Collectively, our study suggests that both PI3-K and MAPK signaling pathways play a significant role in enhanced migration and adhesion of *Nf1* haploinsufficient MSPCs.

**Keywords:** neurofibromatosis 1; neurofibroma; oncogene protein p21 (ras); mesenchymal stem/progenitor cells

---

## 1. Introduction

Neurofibromatosis type 1 (NF1), also known as Von Recklinghausen's disease, is an autosomal dominant disorder with an incidence of 1 in 3000 live births [1]. NF1 is one of the most common genetic disorders with a predilection toward neoplasms, which include astrocytomas, pheochromocytomas, myeloid leukemia, and the pathognomonic cutaneous and plexiform neurofibromas [2]. In addition to these neoplastic conditions, NF1 patients variably experience skeletal deformations, hyperpigmentation of the skin (café-au-lait macules), benign lesions of the iris (Lisch nodules), and intellectual deficits [3,4].

NF1 occurs as a result of mutations in the *NF1* tumor suppressor gene located on chromosome 17p11.2, which encodes a p21ras (Ras) guanosine triphosphatase (GTPase)-activating protein (GAP) called neurofibromin. The neurofibromin GAP domain controls the conversion of Ras-GTP to its inactive GDP-bound state, thereby negatively regulating the activity of downstream signaling pathways, including the mitogen activated protein kinase (MAPK) and phosphoinositide 3-kinase (PI3-K) pathways. Loss of one or both alleles of *NF1* leads to aberrant Ras-dependent cellular functions including proliferation, differentiation, migration, and survival, in multiple cell lineages [5,6].

Mesenchymal stem/progenitor cells (MSPCs) was first isolated from bone marrow by Friedenstein in 1970 [7], follow-up studies demonstrated that they effectively support the hematopoietic stem/progenitor cell (HSPC) functions through expression of adhesion surface molecules, extracellular matrix, and cytokine production within the hematopoietic microenvironment, termed as “niche” [8–11]. MSPCs are identified as being positive for CD105, CD73, CD90, and negative for CD45, CD34 and CD117 [12] and account for 0.01%–0.0001% of all nucleated cells in the bone marrow [13]. MSPCs also retain the capacity for self-renewal and differentiation into many non-hematopoietic mesodermal tissues such as osteoblasts, adipocytes, and chondroblasts *in vitro* [7,14,15] and exhibit the potential to generate complete bone/bone marrow organs *in vivo* [8]. Furthermore, studies have shown that MSPCs produce trophic factors that promote their migration resulting in enhanced tissue repair, thereby providing therapeutic benefit in inflammatory disease processes and sites of injury [16,17]. Skeletal abnormalities, including osteoporosis/osteopenia, osteomalacia, shortness of stature, and macrocephaly are among the common non-malignant complications in patients with NF1, and some of these bone manifestations can result in significant morbidity. Recent studies indicated that the osseous manifestations in NF1 may due to the

impaired maintenance of bone structure and abnormal development of the skeletal system [18–20]. Given that MSPCs are progenitors of osteoblasts, functional defects of MSPCs may be closely relevant to skeletal development.

Our previous studies have shown that heterozygous loss of *Nf1* (*Nf1*<sup>+/-</sup>) in MSPCs led to increased proliferation, hyper activation of p21-Ras and impaired MSPC differentiation into osteoblasts [21]. We have also demonstrated that haploinsufficiency of *Nf1* led to hyper activation of the Ras/PI3-K/MAPK signaling axis in Schwann cells, osteoclasts, and mast cells [22,23]. Till now, the molecular mechanisms underlying the gain-in-migration of NF1 MSPCs remains poorly understood and yet to be elucidated. We hypothesized that *Nf1* heterozygosity may also lead to alteration of MSPC cellular functions including migration and adhesion via p21-Ras mediated hyperactivation of PI3-K or MAPK effector pathways. In the present study, we utilize MSPCs derived from bone marrow of wild-type (WT) and *Nf1*<sup>+/-</sup> mice to investigate whether *Nf1* heterozygosity affects MSPC migration and adhesion capabilities.

## 2. Results

### 2.1. *Nf1*<sup>+/-</sup> MSPCs Have Increased Nuclear-to-Cytoplasmic Ratio

*Nf1*<sup>+/-</sup> MSPCs were noted to have elongated, spindle shaped cytoplasm in comparison to the branched cytoplasm observed in WT MSPCs (Figure 1A). Quantification of this morphological change revealed an increased nuclear-to-cytoplasmic ratio in *Nf1*<sup>+/-</sup> MSPCs compared to WT controls (Figure 1B). These findings indicated involvement of neurofibromin in regulating MSPC morphology.

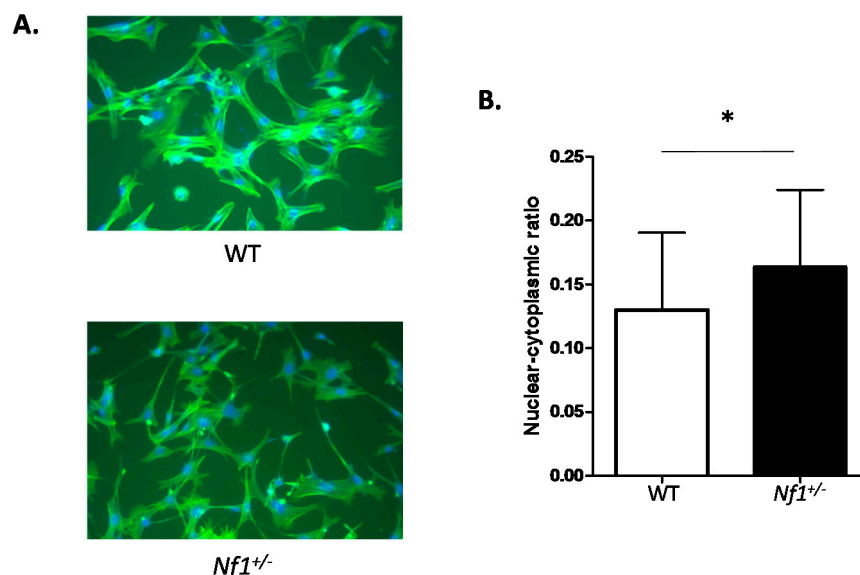


**Figure 1.** Morphological differences between wild-type (WT) and *Nf1* haploinsufficient (*Nf1*<sup>+/-</sup>) mesenchymal stem/progenitor cells (MSPCs). (A) Morphology of WT and *Nf1*<sup>+/-</sup> MSPCs imaged under 200× amplification by phase contrast microscopy. Cells were stained with 400 nM fluorescein isothiocyanate(FITC)-phalloidin and DAPI; (B) A quantitative comparison of nuclear-cytoplasmic ratio between WT and *Nf1*<sup>+/-</sup> MSPCs based on the average ratio of nuclear area/cytoplasm area in 50 cells/field from five different fields. Data are represented as mean ± SD from three batches of MSPCs isolated from individual mice (\* *p* < 0.05 for *Nf1*<sup>+/-</sup> vs. WT MSPCs).

## 2.2. *Nf1*<sup>+/-</sup> MSPCs Have Increased Migratory Capacity

Wound healing assays were performed to assess migration of MSPCs. *Nf1*<sup>+/-</sup> MSPCs were noted to occupy an increased proportion of the wound space as compared to WT MSPCs 24 h after wound formation and continued culture in medium containing 10% fetal bovine serum (FBS) (Figure 2A). Quantification of the wound healing assay revealed a significant increase in the number of migrating *Nf1*<sup>+/-</sup> MSPCs ( $F = 75.76$ ,  $Df = 1$ ,  $p < 0.001$ ; Figure 2B). Actin polymerization was further assessed to determine a molecular basis for the increased migration noted in *Nf1*<sup>+/-</sup> MSPCs. *Nf1*<sup>+/-</sup> MSPCs, as compared to WT controls, demonstrated significantly increased F-actin (polymerized actin) content after FBS stimulation at 30 s (Figure 2C, Figure S1). Taken together, these results suggested an increase in the migratory capacity of *Nf1*<sup>+/-</sup> MSPCs secondary to enhanced F-actin polymerization.

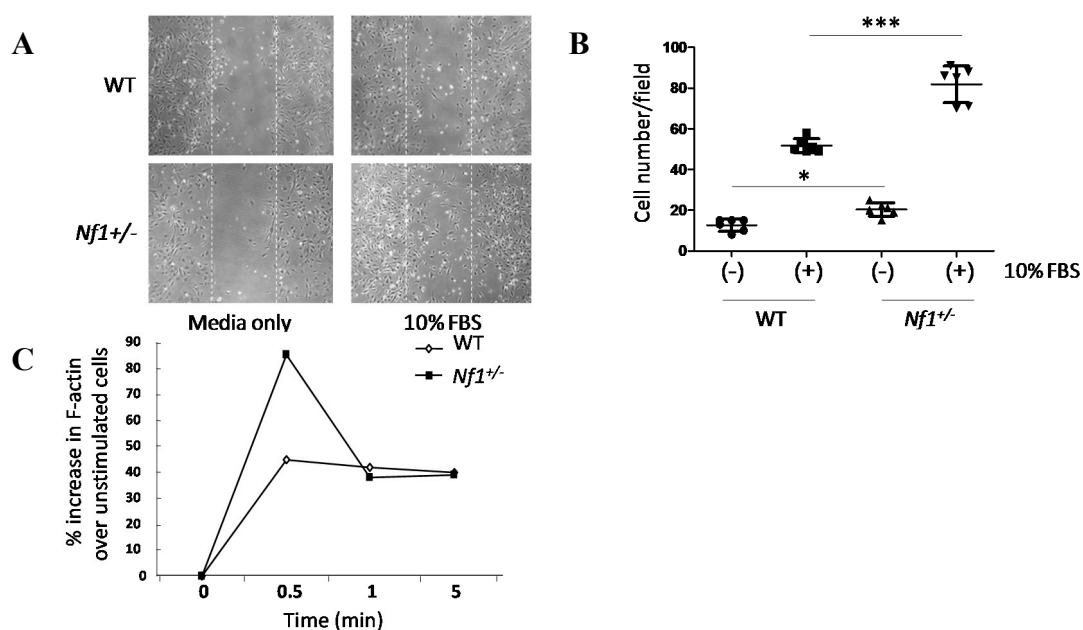


**Figure 2.** Migration and actin polymerization were significantly enhanced in *Nf1*<sup>+/-</sup> MSPCs. (A) Wound healing assays were performed by incubating WT and *Nf1*<sup>+/-</sup> MSPCs in 10  $\mu$ g/mL of mitomycin C for one hour, after which a linear wound (marked by the white dotted lines) was created as shown. Wound healing was allowed to proceed in fresh media for 24 h, (original magnification  $\times 200$ ); (B) The number of cells migrating into the wound field were quantified, revealing an increased migration in *Nf1*<sup>+/-</sup> MSPCs compared with WT MSPCs ( $F = 75.76$ ,  $Df = 1$ ,  $*** p < 0.001$ ;  $*** p < 0.001$  for *Nf1*<sup>+/-</sup> MSPCs vs. WT MSPCs in the presence of 10% FBS,  $* p < 0.05$  for untreated *Nf1*<sup>+/-</sup> MSPCs vs. untreated WT MSPCs). Data are represented as mean  $\pm$  SD from duplicate wells from three independent experiments, each experiment was performed with different MSPCs culture isolated from individual mice; (C) Actin polymerization was measured following 2 h starvation and subsequent treatment with 10% FBS for different time periods. Flow cytometry analysis was performed following 400 nM FITC-phalloidin staining. An increased F-actin content was observed in *Nf1*<sup>+/-</sup> MSPCs comparison to WT MSPCs. A representative result of one of three independent experiments is shown; each experiment was performed with different MSPCs culture isolated from individual mice.

### 2.3. *Nf1* Haploinsufficiency Enhances Cellular Affinity to CH271

*Nf1*<sup>+/-</sup> MSPCs showed significantly increased adhesion to recombinant fibronectin fragment, CH296, pre-coated plates as compared to WT controls (Figure 3A;  $p < 0.001$ , Figure 3B). Fibronectin's binding sites, H296 and CH271, were analyzed for preferential affinity in *Nf1*<sup>+/-</sup> MSPCs. H296 and CH271 specific adhesion assays demonstrated a significant increase in *Nf1*<sup>+/-</sup> MSPC adhesion in CH271 assays but not H296 assays as compared to WT ( $p < 0.001$ , Figure 3C). By contrast, WT MSPCs did not show preference to either CH271 or H296. To further characterize the increased affinity of *Nf1*<sup>+/-</sup> MSPCs for CH271, expression of its receptor, CD49e (also known as integrin  $\alpha 5$  or fibronectin receptor  $\alpha$ ), was quantified by flow cytometry. The expression level of CD49e in *Nf1*<sup>+/-</sup> MSPCs was significantly increased as compared to WT MSPCs (Figure 3D). We also analyzed CD49d, the H296 receptor, and found no statistical difference in expression between WT and *Nf1*<sup>+/-</sup> MSPCs (data not shown).

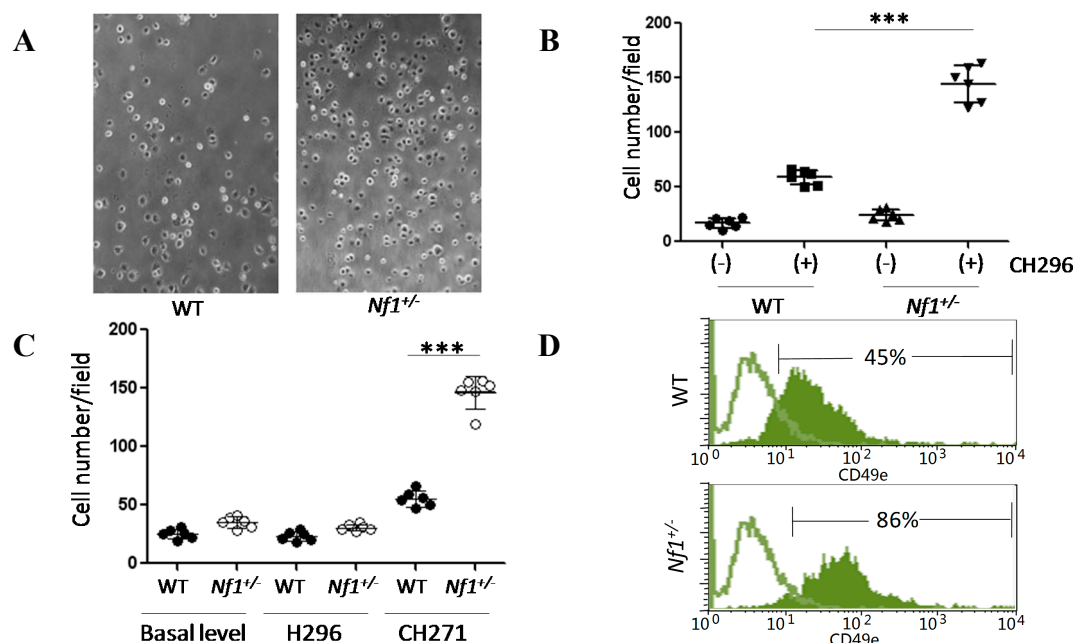


**Figure 3.** Enhancement of cellular adhesion in *Nf1*<sup>+/-</sup> MSPCs. (A) MSPCs were plated into wells pre-coated with either 8  $\mu$ g/mL CH296 (recombinant fibronectin fragment) or 0.1% bovine serum albumin (BSA). Following a 30 min incubation period at 37 °C, the plates were washed and adherent cells were counted on five representative fields/well from six replicate wells, (original magnification  $\times 200$ ); (B) *Nf1*<sup>+/-</sup> MSPCs had significantly increased adhesion to CH296 coated plates in comparison to WT MSPCs (\*\*\*)  $p < 0.001$  for CH296 coated *Nf1*<sup>+/-</sup> MSPCs vs. CH296 coated WT MSPCs); (C) Preferential adhesion to fibronectin binding sites, H296 and CH271, was assessed. *Nf1*<sup>+/-</sup> MSPCs exhibited significantly greater adhesion to CH271 as compared to H296. (\*\*\*)  $p < 0.001$  for CH271 coated *Nf1*<sup>+/-</sup> MSPCs vs. CH271 coated WT MSPCs); (D) Expression of CH271 receptor, CD49e, was quantified by flow cytometry, demonstrating significantly increased expression of CD49e in *Nf1*<sup>+/-</sup> MSPCs in comparison to WT. The green lines represent isotype controls while the green solid areas represent the experimental samples. Data are one representative result of three independent experiments, and each experiment was performed with different MSPCs culture isolated from individual mice.

#### 2.4. Hyper Activation of the PI3-K and MAPK Pathways in *Nf1*<sup>+/-</sup> MSPCs

Serum starved WT and *Nf1*<sup>+/-</sup> MSPCs were stimulated with 10% FBS to assess activation of the PI3-K and MAPK pathways downstream of Ras. Baseline expression of phosphorylated (p) Akt (also known as protein kinase B) and extracellular-signal-regulated protein kinase (Erk) 1/2 in *Nf1*<sup>+/-</sup> and WT MSPCs were undetectable. However, stimulation with 10% FBS for 2 and 5 min showed significantly enhanced expression of pAkt and pErk1/2 in *Nf1*<sup>+/-</sup> MSPCs compared to WT MSPCs. Increased pAkt levels were restored to baseline by 30 min pretreatment of a PI3-K inhibitor, LY294002, in both WT and *Nf1*<sup>+/-</sup> MSPCs. Likewise, pErk1/2 expression was significantly reduced in the presence of a MEK inhibitor, PD0325901, in both WT and *Nf1*<sup>+/-</sup> MSPCs (Figure 4). The pretreatment of LY294002 and PD0325901 has also been prolonged to 4 h, and the results did not show a significant pathway cross talk occurred between these two inhibitors (Figure S2).

Cell viability was not affected by these inhibitors at the concentration applied here. Collectively, these data demonstrated that *Nf1*<sup>+/-</sup> MSPCs exhibit hyperactivation of both the PI3-K and MAPK signaling axes, which can be restored to baseline by pathway specific pharmacologic inhibitors.

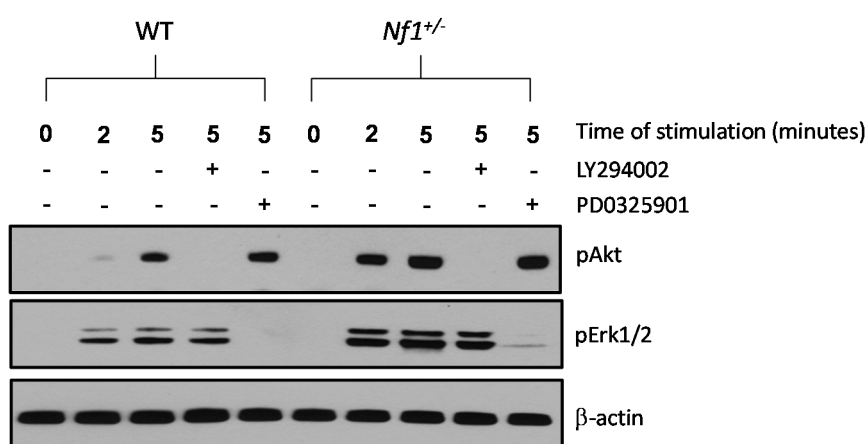


**Figure 4.** *Nf1*<sup>+/-</sup> MSPCs exhibit increased Akt (also known as protein kinase B) and extracellular-signal-regulated protein kinase (Erk)1/2 phosphorylation, which can be inhibited by LY294002 and PD0325901, respectively. Phosphorylation of Akt and Erk1/2 was determined by Western blot in WT and *Nf1*<sup>+/-</sup> MSPCs following 10% FBS stimulation in the presence or absence of PI3-K inhibitor, LY294002, or MAPK inhibitor, PD0325901. Data represents one of three independent experiments, and each experiment was performed with different MSPCs culture isolated from individual mice.

#### 2.5. Enhanced *Nf1*<sup>+/-</sup> MSPCs Migration and Adhesion Is Rescued by LY294002 and PD0325901

In order to determine the functional implications of pharmacologically inhibiting hyperactivated PI3-K and MAPK pathways in *Nf1*<sup>+/-</sup> MSPCs, wound healing and adhesion assays were performed to assess migration and adhesion of MSPCs in the presence of LY294002 or PD0325901 inhibitors. In comparison to WT, *Nf1*<sup>+/-</sup> MSPCs demonstrate increased migration in response to either media alone or media supplemented with 10% FBS, which was significantly attenuated by LY294002 or PD0325901 ( $p < 0.001$ , Figure 5A). Migration of *Nf1*<sup>+/-</sup> MSPCs vs. WT MSPCs responded to different concentrations of PD0325901, as shown in Figure S3. A similar trend was noted in the adhesion assay where *Nf1*<sup>+/-</sup>



MSPCs were significantly more adhesive in comparison to WT in response to either media alone or 10% FBS stimulation. Likewise, adhesion was markedly reduced in the presence of LY294002 and PD0325901 ( $p < 0.001$ , Figure 5B). The efficacy of PI3-K and MAPK inhibitors to significantly attenuate the enhanced signal transduction, migration, and adhesion of MSPCs with *Nf1* haploinsufficiency suggests that these two pathways may play important role in mediating *Nf1*<sup>+/-</sup> MSPC gain-in-functions.

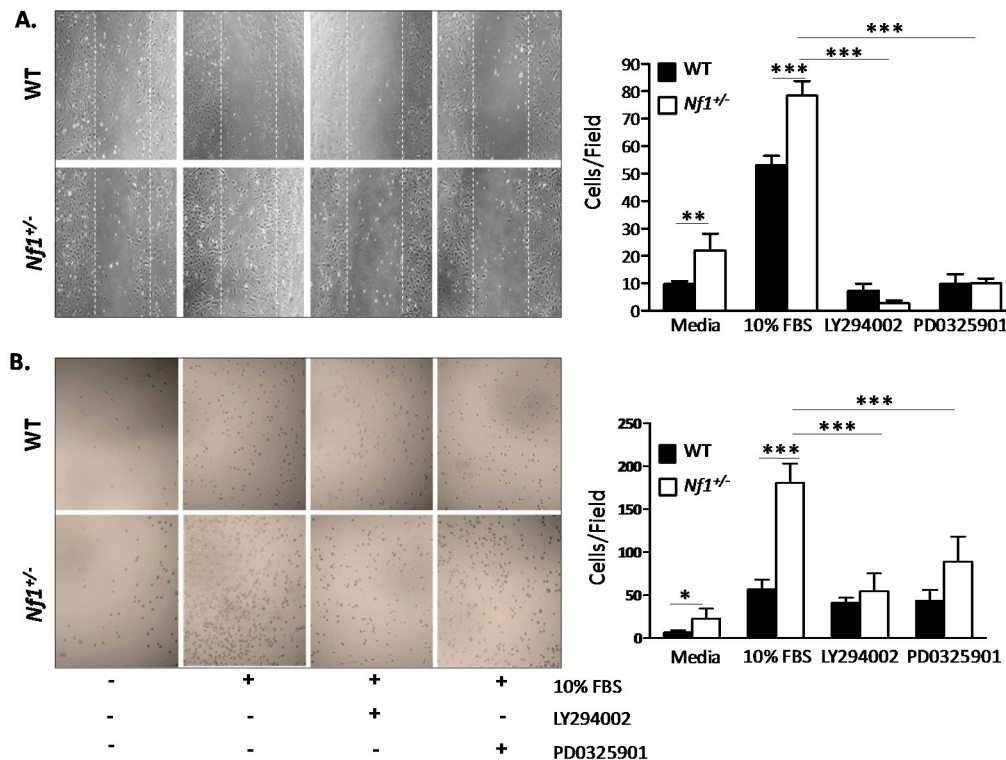


**Figure 5.** Migration and adhesion of *Nf1*<sup>+/-</sup> MSPCs was mediated by mitogen activated protein kinase (MAPK) and phosphoinositide 3-kinase (PI3-K) pathways. **(A)** Representative high power fields (20× objective lens) of wound healing assays for WT and *Nf1*<sup>+/-</sup> MSPCs cultured with serum free media or 10% FBS in the presence or absence of either LY294002 or PD0325901. *Nf1*<sup>+/-</sup> MSPCs have enhanced migration in comparison to WT in serum free or 10% FBS supplemented media, which was significantly decreased by LY294002 and PD0325901 (\*\*  $p < 0.01$  for *Nf1*<sup>+/-</sup> MSPCs vs. WT MSPCs cultured in media; \*\*\*  $p < 0.001$  for 10% FBS treated *Nf1*<sup>+/-</sup> MSPCs vs. 10% FBS treated WT MSPCs; \*\*\*  $p < 0.001$  for LY294002 or PD0325901 treated and untreated *Nf1*<sup>+/-</sup> MSPCs in the presence of 10% FBS); **(B)** Representative high power fields (20× objective lens) from CH296 adhesion assays for WT and *Nf1*<sup>+/-</sup> MSPCs performed in serum free or 10% FBS supplemented media in the presence or absence of LY294002 or PD0325901. The adhesion of *Nf1*<sup>+/-</sup> MSPCs was significantly increased in comparison to WT MSPCs in either serum free or 10% FBS supplemented media. Adhesions were significantly reduced in the presence of LY294002 and PD0325901 (\*  $p < 0.05$  for *Nf1*<sup>+/-</sup> vs. WT MSPCs in serum free media; \*\*\*  $p < 0.001$  for *Nf1*<sup>+/-</sup> vs. WT MSPCs in 10% FBS supplemented media; \*\*\*  $p < 0.001$  for LY294002 or PD0325901 treated and untreated *Nf1*<sup>+/-</sup> MSPCs in the presence of 10% FBS). Data are represented as mean  $\pm$  SD from three individual experiments, and each experiment was performed with different MSPCs culture isolated from individual mice.

### 3. Discussion

NF1 is a heritable or spontaneous autosomal dominant disease, affecting neural tissues, skin, and skeleton. Skeletal abnormalities such as scoliosis, sphenoid wing dysplasia and osteopenia are common manifestations of NF1. Elevated bone resorption has been proven to contribute to the abnormal bone remodeling in NF1 [24]. During bone resorption, the abundant factors released from the bone matrix results in recruitment and differentiation of MSPCs for the following bone remodeling. In addition, fibroblasts are one of the major cell components of neurofibromas. Through current studies indicated that endoneurial fibroblasts are neural crest derivative [25], whereas perineurial fibroblasts, which are involved in the nerve degeneration and regeneration of NF1, are mesenchymal origin [26,27]. Nevertheless, the relevance between MSPCs and fibroblasts in neurofibromas still needs further investigation. Taken together, MSPCs and its progeny cells may play a critical role in the pathogenesis of NF1.

Just like HSPCs, MSPCs migrate and localize throughout the whole body. Several studies have demonstrated migratory capabilities of MSPCs are mediated through numerous chemokine-receptor interactions and cell adhesion molecules [11,28–32]. Takashima and colleagues have reported the presence of neuroepithelium-derived and neural crest-derived MSPCs in cell populations of femoral and tibial bones in postnatal mice [33]. A study performed by Mansilla *et al.* indicated that peripheral blood collected from a group of 15 acute burn victims showed a larger percentage of MSPCs compared to a group of 15 healthy individuals [34]. Collectively, these studies demonstrated the migratory capabilities of MSPCs and implicated their involvement in the regenerative process *in vivo*. However, little is known about the molecular mechanism(s) underlying MSPC migration under the circumstance of NF1, which may further inform the role of MSPCs in the pathogenesis of NF1 such as abnormal bone remodeling and tissue repair.

Ponte *et al.* [35] have shown that bone marrow MSPCs have the tendency to migrate towards certain growth factors and chemokines when cultured *in vitro*. Using transwell migration assay, platelet derived growth factor (PDGF) was demonstrated to have the most potent MSPC attractive effect. Other studies have shown that when plated with vascular smooth muscle cells, PDGF induces an increase in MAPK activity [36]. As an inflammatory cytokine, tumor necrosis factor- $\alpha$  (TNF- $\alpha$ ) is known to significantly increase Ras activity [37]. Furthermore, TNF- $\alpha$  mediated stimulation of bone marrow MSPCs was shown to improve their response to certain chemokines such as stromal cell derived factor 1 (SDF-1) and RANTES and enhance migratory functions compared to non-stimulated control [38]. These aforementioned studies implicate a critical role for Ras and its downstream signaling pathway in MSPC migratory functions. We hypothesized that hyperactivation of p21-Ras pivotally underpins the enhanced cellular adhesion and migratory functions of *Nf1*<sup>+/-</sup> MSPCs. *Nf1*<sup>+/-</sup> MSPCs demonstrate hyperactivation of p21 Ras secondary to neurofibromin haploinsufficiency. The MAPK and PI3-K pathways are direct downstream effectors of p21-Ras. In our study, hyperactivity of the PI3-K and MAPK pathways in *Nf1*<sup>+/-</sup> MSPCs was confirmed by Western blot demonstrating increased levels of pAkt and pErk1/2. Through the adhesion and wound healing assays, we have shown that *Nf1*<sup>+/-</sup> MSPCs exhibit significantly enhanced adhesion and migration capabilities compared to WT MSPCs. Furthermore, inhibition of MAPK and PI3-K pathways in *Nf1*<sup>+/-</sup> MSPCs using PD0325901 or LY294002, respectively, resulted in a dramatic decrease in the enhanced migratory



and adhesive capacity of *Nf1*<sup>+/-</sup> MSPCs to levels comparable to WT cells. Similarly, transwell migration assay also showed the enhanced migration in *Nf1*<sup>+/-</sup> MSPCs was restored to the same level as WT MSPCs in the presence of PD0325901 or LY294002 (Figure S4). However, Koivunen *et al.* [39] demonstrated that neither the function of wound healing nor the Ras-MAPK activity were enhanced in epidermal cells of NF1 patients, indicated that NF1 gene play a key regulator of Ras signaling only in some kinds of cell types.

Studies have also demonstrated that Ras signaling regulated *Nf1* heterozygous cell migration in other cell types, indicating that the defects of cell motility may be a common characteristic of neurofibromin deficiency. Neurofibromin-deficient macrophages demonstrated increased proliferation, migration, and adhesion, which were regulated by Ras-MAPK signaling [40]. Similarly, osteoclasts derived from NF1 patients demonstrated increased migration and adhesion capacity associated with hyperactivity of MAPK pathways [41]. While in *Nf1*<sup>-/-</sup> Schwann cells, not only MAPK but also PI3-K pathways contributed to the increased migration capacity [42], which was consistent with our results in this study, implying synergistic effect of these two pathways in the migratory phenotype in certain cell types. In addition to the impaired osteoblastic differentiation reported by us previously, the enhanced migration and adhesion in MSPCs may also be associated with the osseous manifestations in NF1 patients.

## 4. Experimental Section

### 4.1. Animals and Materials

*Nf1* mice were obtained from Dr. Tyler Jacks at the Massachusetts Institute of Technology (Cambridge, MA, USA) in a C57BL/6J.129 background and backcrossed for 13 generations into a C57BL/6J strain. *Nf1*<sup>+/-</sup> mice were genotyped by polymerase chain reaction (PCR) as previously described [22]. These studies were conducted with a protocol approved by the Indiana University Laboratory Animal Research Center using four to eight week old WT and *Nf1*<sup>+/-</sup> mice.

### 4.2. Isolation and Expansion of MSPCs

MSPCs were generated from WT and *Nf1*<sup>+/-</sup> mice as previously described [43]. Briefly, four to eight week old WT and *Nf1*<sup>+/-</sup> mice were sacrificed by CO<sub>2</sub> inhalation followed by cervical dislocation. Bone marrow cells were collected by flushing the femurs and tibias with Iscove's Modified Dulbecco's Medium (IMDM, Gibco-invitrogen, Carlsbad, CA, USA) containing 2% FBS using a 23-gauge needle. Bone marrow mononuclear cells (BMMNCs) were then separated by low-density gradient centrifugation using Ficoll Hypaque. Cells were washed twice with IMDM and suspended in mouse MesenCult basal medium containing mesenchymal cell stimulating supplements (Stem Cell Technologies Inc., Vancouver, BC, Canada). The cells were then plated at a density of  $2 \times 10^7$  cells in a 10-cm tissue culture dish (BD Falcon, Franklin Lakes, NJ, USA).

### 4.3. Phenotypic Analysis of MSPCs

The expression of cell surface markers were analyzed to measure the purity of the cultured MSPCs. One hundred thousand cells were re-suspended in 100  $\mu$ L of 0.1% BSA/PBS and stained with FITC-anti-mouse CD44, R-phycoerythrin (R-PE)-conjugated anti-mouse CD49e, R-PE-conjugated

anti-mouse CD29, purified rat anti-mouse CD105, anti-rat R-PE antibody, c-Kit, CD34, CD13, Mac-1, B220, and Gr-1 antibodies (BD Pharmingen, San Diego, CA, USA) for 30 min at 4 °C. After washing with PBS twice, the labeled cells were analyzed via flow cytometry (Becton-Dickinson, San Jose, CA, USA).

#### 4.4. Cellular Morphology

Morphological analysis was determined by plating  $1 \times 10^4$  cells/well in a plastic 8-well chamber slide (Ibidi, Martinsried, Germany) for 24 h in MesenCult media with supplemental added. Cells were then fixed with 3.7% formaldehyde and permeabilized with 0.1% Triton X/PBS for 5 min and blocked for 1 h in 5% Milk/PBS before staining with DAPI and 400nM FITC-phalloidin (Sigma P5282, St. Louis, MO, USA). Cells were examined and images were acquired using deconvolution microscope (Delta vision Elite, Applied Precision, Mississauga, ON Canada). Average ratio of nuclear to cytoplasmic areas was calculated using ImageJ software (NIH, Cambridge, MA, USA).

#### 4.5. Actin Polymerization

Actin polymerization was measured as described previously [38]. Briefly, Cells were starved for 2 h and then treated with or without 10% FBS for 30 s, 1 min and 5 min and fixed with 3.7% formaldehyde in PBS and stained with 400 nM FITC phalloidin (Sigma P5282). Cells were then incubated for 10 min at 37 °C and transferred to 4 °C for overnight staining. The following day, cells were washed and analyzed by flow cytometer (Becton-Dickinson).

#### 4.6. Adhesion Assay

MSPCs were starved in DMEM for 2 h, detached with trypsin, washed, and resuspended in serum-free media with 0.01% BSA, and then plated in pre-coated plates containing 8 µg/mL CH296, 30 µg/mL CH271 or 20 µg/mL H296 (Takara Bio., Otsu, Japan). The cells were allowed to attach and spread for 1 h at 37 °C, and then unbound cells were removed by gentle washing with PBS. Attached cells were fixed with 10% formaldehyde, stained with 0.1% crystal violet and counted [44].

#### 4.7. Wound Healing Assay

The migratory ability of MSPCs was measured using a wound-healing assay [45]. In brief,  $1 \times 10^5$  cells were plated on BD Falcon 12-well tissue culture plates at approximately 70% confluence. A wound was then created by scratching a linear ridge in the cell monolayer using a 1000 µL pipette tip (approximately 1.3 mm wide), ensuring that all wounds were of equivalent width. To prevent width change secondary to cellular proliferation, MSPC cultures were treated with 10 µg/mL of mitomycin C (Sigma M7949) 1 h prior to wound formation to block cellular mitosis. In experiments with inhibitors, LY294002 (10 µM) or PD0325901 (100 nM), cells were co-incubated for 1 h with mitomycin C. Upon wound generation, cell culture media was replaced with fresh media, and wound closure was allowed to proceed for 24 h prior to Hema-3 staining (Fisher Scientific Company LLC, Kalamazoo, MI, USA).

#### 4.8. Western Blot

WT and *Nf1*<sup>+/-</sup> MSPCs were deprived of serum and growth factors for 24 h. For the stimulation only group, cells were stimulated with 10% FBS for 2 or 5 min. For the inhibitor group, cells were pre-incubated with LY294002 (10  $\mu$ M) or PD0325901 (100 nM) for 30 min, followed by stimulation with 10% FBS for 5 min. Cells were lysed in nonionic lysis buffer (20 mM Tris-Cl, 137 mM NaCl, 1 mM EGTA (ethylene-glycol-tetra-acetic acid), 1% Triton X-100, 10% glycerol, 1.5 mM MgCl<sub>2</sub>) containing protease and phosphatase inhibitors (Amersham Pharmacia Biotech, Piscataway, NJ, USA). The protein concentration of the lysates was normalized using a bicinchoninic acid (BCA) assay kit (Pierce, Rockford, IL, USA). Proteins were separated by 12.5% sodium dodecyl sulfate polyacrylamide gel electrophoresis (SDS-PAGE) and transferred to high-quality polyvinylidene difluoride membranes (Roche Diagnostics, Indianapolis, IN, USA) in a Tris (20 mM), glycine (150 mM) and methanol (20%) buffer at 250 mV for 2 h. After blocking in 5% nonfat dry milk in phosphate buffered saline tween-20 (PBST), the membranes were incubated with primary antibodies at 1:1000 dilution (phospho-Erk, phospho-Akt,  $\beta$ -Actin; Cell Signaling, Danvers, MA, USA) in 5% milk in PBST overnight at 4 °C. Following overnight exposure, the membranes were washed three times with PBST and incubated with secondary antibodies (anti-rabbit, anti-mouse, GE Healthcare UK Limited, UK) conjugated with horseradish peroxidase at 1:5000 dilution in 5% milk in PBST for 1 h at room temperature. Membranes were washed again in PBST three times at room temperature. Membranes were exposed to SuperSignal West Pico Chemiluminescent Substrate (Thermo Scientific, Rockford, IL, USA) and protein bands were visualized on an X-ray film (GeneMate, Kaysville, UT, USA).

#### 4.9. Statistical Analysis

All statistical analyses were performed with GraphPad Prism 5.0. Unpaired two-tailed student's *t* tests were used for two variable comparisons. Two-way ANOVA with Bonferroni *post-hoc* corrections was performed for experiments with two different categorical independent variables. Data are presented as mean  $\pm$  SD. The number of biologically-independent replicates, and significance levels were shown in the figure legends. Differences were considered statistically significant at  $p < 0.05$ .

### 5. Conclusions

In sum, these data indicated a critical role for *Nf1* in regulating multiple MSPCs functions, including migration and adhesion through both the PI3-K and MAPK pathways. Inhibition of these hyperactive pathways independently in *Nf1*<sup>+/-</sup> MSPCs resulted in attenuation of their enhanced propensity to migrate and adhere. Further characterization of the role of PI3-K and MAPK signal transduction in MSPC function is of critical importance to providing continued insight into the homing and migratory capabilities of MSPCs with potential future therapeutic applications.

#### Supplementary Materials

Supplementary materials can be found at <http://www.mdpi.com/1422-0067/16/06/12345/s1>.

## Acknowledgments

We thank Heather Daniel for administrative support. This work was supported by the Department of Defense (NF100087), National Natural Science Foundation of China (81270575, 81328003, and 81170512).

## Author Contributions

Yuan Zhou, Yongzheng He, Xiaohua Wu and Selina A. Estwick performed experiments. Yuan Zhou, Wen Xing and Feng-Chun Yang analyzed data. Yuan Zhou, Mingjiang Xu and Feng-Chun Yang wrote the manuscript. Richa Sharma and Steven D. Rhodes critically revised the manuscript.

## Conflicts of Interest

The authors declare no conflict of interest.

## References

1. Friedman, J.M.; Birch, P.H. Type 1 neurofibromatosis: A descriptive analysis of the disorder in 1728 patients. *Am. J. Med. Genet.* **1997**, *70*, 138–143.
2. Szudek, J.; Birch, P.; Riccardi, V.M.; Evans, D.G.; Friedman, J.M. Associations of clinical features in neurofibromatosis 1 (NF1). *Genet. Epidemiol.* **2000**, *19*, 429–439.
3. Riccardi, V.M. Neurofibromatosis: Past, present, and future. *N. Engl. J. Med.* **1991**, *324*, 1283–1285.
4. Goldberg, Y.; Dibbern, K.; Klein, J.; Riccardi, V.M.; Graham, J.M., Jr. Neurofibromatosis type 1—An update and review for the primary pediatrician. *Clin. Pediatr.* **1996**, *35*, 545–561.
5. Bourne, H.R.; Sanders, D.A.; McCormick, F. The GTPase superfamily: A conserved switch for diverse cell functions. *Nature* **1990**, *348*, 125–132.
6. Hall, A. The cellular functions of small GTP-binding proteins. *Science* **1990**, *249*, 635–640.
7. Friedenstein, A.J.; Chailakhjan, R.K.; Lalykina, K.S. The development of fibroblast colonies in monolayer cultures of guinea-pig bone marrow and spleen cells. *Cell Tissue Kinet.* **1970**, *3*, 393–403.
8. Sacchetti, B.; Funari, A.; Michienzi, S.; di Cesare, S.; Piersanti, S.; Saggio, I.; Tagliafico, E.; Ferrari, S.; Robey, P.G.; Riminucci, M.; *et al.* Self-renewing osteoprogenitors in bone marrow sinusoids can organize a hematopoietic microenvironment. *Cell* **2007**, *131*, 324–336.
9. Mendez-Ferrer, S.; Michurina, T.V.; Ferraro, F.; Mazloom, A.R.; Macarthur, B.D.; Lira, S.A.; Scadden, D.T.; Ma'ayan, A.; Enikolopov, G.N.; Frenette, P.S. Mesenchymal and haematopoietic stem cells form a unique bone marrow niche. *Nature* **2010**, *466*, 829–834.
10. Bianco, P. Bone and the hematopoietic niche: A tale of two stem cells. *Blood* **2011**, *117*, 5281–5288.
11. Honczarenko, M.; Le, Y.; Swierkowski, M.; Ghiran, I.; Glodek, A.M.; Silberstein, L.E. Human bone marrow stromal cells express a distinct set of biologically functional chemokine receptors. *Stem Cells* **2006**, *24*, 1030–1041.

12. Dominici, M.; le Blanc, K.; Mueller, I.; Slaper-Cortenbach, I.; Marini, F.; Krause, D.; Deans, R.; Keating, A.; Prockop, D.; Horwitz, E. Minimal criteria for defining multipotent mesenchymal stromal cells. The International Society for Cellular Therapy position statement. *Cytotherapy* **2006**, *8*, 315–317.
13. Ma, S.; Xie, N.; Li, W.; Yuan, B.; Shi, Y.; Wang, Y. Immunobiology of mesenchymal stem cells. *Cell Death Differ.* **2014**, *21*, 216–225.
14. Friedenstein, A.J. Marrow stromal fibroblasts. *Calcif. Tissue Int.* **1995**, *56*, S17.
15. Friedenstein, A.J.; Chailakhyan, R.K.; Gerasimov, U.V. Bone marrow osteogenic stem cells: *In vitro* cultivation and transplantation in diffusion chambers. *Cell Tissue Kinet.* **1987**, *20*, 263–272.
16. Bai, L.; Lennon, D.P.; Caplan, A.I.; DeChant, A.; Hecker, J.; Kranso, J.; Zaremba, A.; Miller, R.H. Hepatocyte growth factor mediates mesenchymal stem cell-induced recovery in multiple sclerosis models. *Nat. Neurosci.* **2012**, *15*, 862–870.
17. Ren, G.; Zhang, L.; Zhao, X.; Xu, G.; Zhang, Y.; Roberts, A.I.; Zhao, R.C.; Shi, Y. Mesenchymal stem cell-mediated immunosuppression occurs via concerted action of chemokines and nitric oxide. *Cell Stem Cell* **2008**, *2*, 141–150.
18. Kuorilehto, T.; Poyhonen, M.; Bloigu, R.; Heikkinen, J.; Vaananen, K.; Peltonen, J. Decreased bone mineral density and content in neurofibromatosis type 1: Lowest local values are located in the load-carrying parts of the body. *Osteoporos. Int.* **2005**, *16*, 928–936.
19. Illes, T.; Halmai, V.; de Jonge, T.; Dubousset, J. Decreased bone mineral density in neurofibromatosis-1 patients with spinal deformities. *Osteoporos. Int.* **2001**, *12*, 823–827.
20. Lammert, M.; Kappler, M.; Mautner, V.F.; Lammert, K.; Storkel, S.; Friedman, J.M.; Atkins, D. Decreased bone mineral density in patients with neurofibromatosis 1. *Osteoporos. Int.* **2005**, *16*, 1161–1166.
21. Wu, X.; Estwick, S.A.; Chen, S.; Yu, M.; Ming, W.; Nebesio, T.D.; Li, Y.; Yuan, J.; Kapur, R.; Ingram, D.; *et al.* Neurofibromin plays a critical role in modulating osteoblast differentiation of mesenchymal stem/progenitor cells. *Hum. Mol. Genet.* **2006**, *15*, 2837–2845.
22. Yang, F.C.; Ingram, D.A.; Chen, S.; Hingtgen, C.M.; Ratner, N.; Monk, K.R.; Clegg, T.; White, H.; Mead, L.; Wenning, M.J.; *et al.* Neurofibromin-deficient Schwann cells secrete a potent migratory stimulus for *Nfl*<sup>+/-</sup> mast cells. *J. Clin. Investig.* **2003**, *112*, 1851–1861.
23. Yang, F.C.; Chen, S.; Clegg, T.; Li, X.; Morgan, T.; Estwick, S.A.; Yuan, J.; Khalaf, W.; Burgin, S.; Travers, J.; *et al.* *Nfl*<sup>+/-</sup> mast cells induce neurofibroma like phenotypes through secreted TGF- $\beta$  signaling. *Hum. Mol. Genet.* **2006**, *15*, 2421–2437.
24. Stevenson, D.A.; Schwarz, E.L.; Viskochil, D.H.; Moyer-Mileur, L.J.; Murray, M.; Firth, S.D.; D'Astous, J.L.; Carey, J.C.; Pasquali, M. Evidence of increased bone resorption in neurofibromatosis type 1 using urinary pyridinium crosslink analysis. *Pediatr. Res.* **2008**, *63*, 697–701.
25. Joseph, N.M.; Mukouyama, Y.S.; Mosher, J.T.; Jaegle, M.; Crone, S.A.; Dormand, E.L.; Lee, K.F.; Meijer, D.; Anderson, D.J.; Morrison, S.J. Neural crest stem cells undergo multilineage differentiation in developing peripheral nerves to generate endoneurial fibroblasts in addition to Schwann cells. *Development* **2004**, *131*, 5599–5612.
26. Rosenbaum, T.; Boissy, Y.L.; Kombrinck, K.; Brannan, C.I.; Jenkins, N.A.; Copeland, N.G.; Ratner, N. Neurofibromin-deficient fibroblasts fail to form perineurium *in vitro*. *Development* **1995**, *121*, 3583–3592.

27. Cichowski, K.; Jacks, T. *NF1* tumor suppressor gene function: Narrowing the GAP. *Cell* **2001**, *104*, 593–604.
28. Son, B.R.; Marquez-Curtis, L.A.; Kucia, M.; Wysoczynski, M.; Turner, A.R.; Ratajczak, J.; Ratajczak, M.Z.; Janowska-Wieczorek, A. Migration of bone marrow and cord blood mesenchymal stem cells *in vitro* is regulated by stromal-derived factor-1-CXCR4 and hepatocyte growth factor-c-met axes and involves matrix metalloproteinases. *Stem Cells* **2006**, *24*, 1254–1264.
29. Forte, G.; Minieri, M.; Cossa, P.; Antenucci, D.; Sala, M.; Gnocchi, V.; Fiaccavento, R.; Carotenuto, F.; de Vito, P.; Baldini, P.M.; *et al.* Hepatocyte growth factor effects on mesenchymal stem cells: Proliferation, migration, and differentiation. *Stem Cells* **2006**, *24*, 23–33.
30. Ball, S.G.; Shuttleworth, C.A.; Kielty, C.M. Vascular endothelial growth factor can signal through platelet-derived growth factor receptors. *J. Cell Biol.* **2007**, *177*, 489–500.
31. Palumbo, R.; Galvez, B.G.; Pusterla, T.; de Marchis, F.; Cossu, G.; Marcu, K.B.; Bianchi, M.E. Cells migrating to sites of tissue damage in response to the danger signal HMGB1 require NF- $\kappa$ B activation. *J. Cell Biol.* **2007**, *179*, 33–40.
32. Balkwill, F. Cancer and the chemokine network. *Nat. Rev. Cancer* **2004**, *4*, 540–550.
33. Takashima, Y.; Era, T.; Nakao, K.; Kondo, S.; Kasuga, M.; Smith, A.G.; Nishikawa, S. Neuroepithelial cells supply an initial transient wave of MSC differentiation. *Cell* **2007**, *129*, 1377–1388.
34. Mansilla, E.; Marin, G.H.; Drago, H.; Sturla, F.; Salas, E.; Gardiner, C.; Bossi, S.; Lamonega, R.; Guzman, A.; Nunez, A.; *et al.* Bloodstream cells phenotypically identical to human mesenchymal bone marrow stem cells circulate in large amounts under the influence of acute large skin damage: New evidence for their use in regenerative medicine. *Transpl. Proc.* **2006**, *38*, 967–969.
35. Ponte, A.L.; Marais, E.; Gallay, N.; Langonne, A.; Delorme, B.; Herault, O.; Charbord, P.; Domenech, J. The *in vitro* migration capacity of human bone marrow mesenchymal stem cells: Comparison of chemokine and growth factor chemotactic activities. *Stem Cells* **2007**, *25*, 1737–1745.
36. Kingsley, K.; Plopper, G.E. Platelet-derived growth factor modulates rat vascular smooth muscle cell responses on laminin-5 via mitogen-activated protein kinase-sensitive pathways. *Cell Commun. Signal.* **2005**, *3*, 2.
37. Muller, G.; Storz, P.; Bourteele, S.; Doppler, H.; Pfizenmaier, K.; Mischak, H.; Philipp, A.; Kaiser, C.; Kolch, W. Regulation of Raf-1 kinase by TNF via its second messenger ceramide and cross-talk with mitogenic signalling. *EMBO J.* **1998**, *17*, 732–742.
38. Yang, F.C.; Kapur, R.; King, A.J.; Tao, W.; Kim, C.; Borneo, J.; Breese, R.; Marshall, M.; Dinauer, M.C.; Williams, D.A. Rac2 stimulates Akt activation affecting BAD/Bcl-XL expression while mediating survival and actin function in primary mast cells. *Immunity* **2000**, *12*, 557–568.
39. Koivunen, J.; Karvonen, S.L.; Yla-Outinen, H.; Aaltonen, V.; Oikarinen, A.; Peltonen, J. NF1 tumor suppressor in epidermal wound healing with special focus on wound healing in patients with type 1 neurofibromatosis. *Arch. Dermatol. Res.* **2005**, *296*, 547–554.
40. Stansfield, B.K.; Bessler, W.K.; Mali, R.; Mund, J.A.; Downing, B.D.; Kapur, R.; Ingram, D.A., Jr. Ras-Mek-Erk signaling regulates Nfl heterozygous neointima formation. *Am. J. Pathol.* **2014**, *184*, 79–85.



41. Stevenson, D.A.; Yan, J.; He, Y.; Li, H.; Liu, Y.; Zhang, Q.; Jing, Y.; Guo, Z.; Zhang, W.; Yang, D.; *et al.* Multiple increased osteoclast functions in individuals with neurofibromatosis type 1. *Am. J. Med. Genet. Part A* **2011**, *155A*, 1050–1059.
42. Huang, Y.; Rangwala, F.; Fulkerson, P.C.; Ling, B.; Reed, E.; Cox, A.D.; Kamholz, J.; Ratner, N. Role of TC21/R-Ras2 in enhanced migration of neurofibromin-deficient Schwann cells. *Oncogene* **2004**, *23*, 368–378.
43. Meirelles Lda, S.; Nardi, N.B. Murine marrow-derived mesenchymal stem cell: Isolation, *in vitro* expansion, and characterization. *Br. J. Haematol.* **2003**, *123*, 702–711.
44. Loughran, G.; Healy, N.C.; Kiely, P.A.; Huigsloot, M.; Kedersha, N.L.; O'Connor, R. Mystique is a new insulin-like growth factor-I-regulated PDZ-LIM domain protein that promotes cell attachment and migration and suppresses Anchorage-independent growth. *Mol. Biol. Cell* **2005**, *16*, 1811–1822.
45. Javelaud, D.; Laboureaud, J.; Gabison, E.; Verrecchia, F.; Mauviel, A. Disruption of basal JNK activity differentially affects key fibroblast functions important for wound healing. *J. Biol. Chem.* **2003**, *278*, 24624–24628.

© 2015 by the authors; licensee MDPI, Basel, Switzerland. This article is an open access article distributed under the terms and conditions of the Creative Commons Attribution license (<http://creativecommons.org/licenses/by/4.0/>).